Achievements and challenges in thin film silicon module production

B. Stannowski [a,*], O. Gabriel [a], S. Calnan [a], T. Frijnts [b], A. Heidelberg [b], S. Neubert [a], S. Kirner [a], S. Ring [a], M. Zelt [a], B. Rau [a], J.-H. Zollondz [b], H. Bloess [b], R. Schlatmann [a], B. Rech [a]

[a] Helmholtz-Zentrum Berlin für Materialien und Energie, PVcomB, Schwarzschildstr. 3, 12489 Berlin, Germany
[b] Masdar PV GmbH, 99334 Ichtershausen, Germany

ARTICLE INFO

ABSTRACT

This paper addresses the achievements and challenges in a-Si:H/μc-Si:H tandem solar cell technology including production aspects. As an example we show figures of the module production at Masdar PV, with module conversion efficiencies reaching 10%. The process integration was supported by PVcomB, namely, by developing improved PECVD processes and transferring them to Masdar PV. The important role of the TCO substrate for producing high-efficiency modules at lowest possible costs is discussed. We show the results of tandem cells on thermally annealed ZnO:Al substrates, resulting in an improvement of 0.4–0.5% (abs) as a result of the TCO annealing, reaching a stable efficiency of 12.1% for a 1 cm² solar cell and 11.6% for a mini module. The challenges in developing thin film silicon solar modules with higher efficiency than presently reached are discussed.

© 2013 Elsevier B.V. All rights reserved.

1. Introduction

The photovoltaic (PV) market has grown continuously over the past years with a cumulated capacity installed worldwide reaching 100 gigawatt-peak to date [1]. As a consequence, module sales prices have dropped tremendously. A trend that is expected to continue, driving module prices and production costs further down. Crystalline silicon (c-Si) based modules are dominating the market with a share of more than 85% [2]. Thin film modules based on amorphous silicon (a-Si:H) and microcrystalline silicon (μc-Si:H), copper–indium–gallium–diselenide (CIGS), or cadmium–telluride (CdTe) are considered an alternative to reduce costs, energy pay-back time, and the consumption of raw materials. With conversion efficiencies of commercial modules being in the range of 8–13% as compared to 14–20% for c-Si based modules, however, these modules need lower production costs in order to compensate for higher PV system mounting costs.

Thin-film silicon modules, such as a-Si:H based modules, are an ideal option for a future terawatt PV market since such modules are based on non-toxic materials and all raw materials are available in practically unlimited quantities [3]. They are ideal for application in large-scale power plants, preferably in hot regions. The lower mounting costs for such power plants are more favorable for modules with lower efficiency. For application in hot regions with higher module operating temperatures the energy output of a-Si:H based module is favorable with respect to c-Si based modules due to the lower temperature coefficient [4]. Additionally, the light-induced

degradation of such modules is lower at elevated temperatures [5,6]. Moreover, thin film silicon modules are ideal candidates for building-integrated photovoltaics (BIPV) due to the homogeneous, dark appearance and the flexibility in module size up to 5.7 m². The low temperature coefficient favors high output in BIPV applications. The possibility in producing semi-transparent modules by laser scribing, and the use of non-toxic raw materials make thin film silicon attractive for BIPV.

This paper addresses a-Si:H/μc-Si:H tandem junctions. An introduction and overview to this technology can be found in [7–9]. After the first a-Si:H/μc-Si:H ("micromorph") solar cells were reported in 1996 by Meier et al. [10], Kaneka was the first company developing high efficiency tandem and triple cells with currently up to 12.3% stable efficiency [11–13] and started large-scale module production around ten years ago [14]. In the past few years many companies established production lines with module efficiencies continuously being increased to currently up to 9–10% in production average and module size up to 5.7 m² [15]. Prototype modules on production scale reach stabilized efficiencies close to 11% based on a tandem junction [16,17] or a triple junction [18]. These values are remarkably close to the best solar cell efficiencies of up to 12.3% obtained in laboratories with tandem junctions [11,19–23] and, recently reported by LG Electronics, 13.4% with an a-Si:H/μc-Si:H/μc-Si:H triple junction [18,24]. It demonstrates the mature processes and production equipment benefitting from the flat panel display industry, on the one hand side, but also the urgent need to push up the laboratory efficiencies on the other hand side. The low module efficiency is the most severe restraint and a potential show stopper for this technology if no new concepts for higher efficiencies are developed.

As one of the largest producers of a-Si:H/μc-Si:H tandem modules, Masdar PV GmbH operates a sunfab-type production

* Corresponding author. Tel.: +49 30 806215491; fax: +49 30 806215677.
E-mail address: bernd.stannowski@helmholtz-berlin.de (B. Stannowski).

line from Applied Materials with a name plate capacity of 95 MW$_p$. With a-Si:H single junction based modules reaching stabilized efficiencies of 8% produced first, the production was changed to a-Si:H/μc-Si:H tandem modules in August 2011. As a cooperation partner of Masdar PV the Competence Center Thin-Film and Nano-technology for Photovoltaics Berlin (PVcomB) offers a platform for technology development and process transfer for thin-film PV modules. For this purpose two R & D lines for a-Si:H/μc-Si:H and CIGS based modules on 30 × 30 cm^2 are operated. In this paper we present results from process transfer of a-Si:H/μc-Si:H modules from PVcomB to production at Masdar PV yielding modules with 10% stable efficiency on 5.7 m² size. As an example for joint R & D work on solar cells with higher efficiency we present results of tandem cells on thermally annealed aluminum doped zinc oxide (ZnO:Al). We conclude with discussing the perspectives for a-Si:H/μc-Si solar cells and modules.

2. Process transfer from PVcomB to Masdar PV

The silicon deposition equipment of the a-Si:H/μc-Si:H tandem lines at PVcomB and Masdar PV are plasma-enhanced chemical vapor deposition (PECVD) cluster tools from Applied Materials, AKT1600 (Gen 2) and AKT60K (Gen 8.5), respectively. Both are operated at a plasma excitation frequency of 13.56 MHz. The production line consists of four AKT60K cluster tools with seven deposition chambers each and a substrate size of 5.7 m². Generally, one tool is used for deposition of the a-Si:H top cell and three tools are used for the μc-Si:H bottom cell. The use of similar PECVD platforms facilitates fast process transfer from PVcomB to the production at Masdar PV.

At PVcomB the fully automated AKT1600 cluster tool is equipped with three process chambers for a substrate size up to 30 × 30 cm^2. This allows for separation of the deposition of doped and intrinsic materials and processing of 6–8 tandem modules per day. In-situ and remote plasma cleaning by NF$_3$ is used for chamber cleaning. To support the PECVD process development, a number of in situ diagnostic tools are installed, such as optical emission spectroscopy (OES) and mass spectrometry (residual gas analyzer, RGA). Aluminum doped zinc oxide (ZnO:Al) front and

ZnO:Al/Ag back contacts are deposited in an in-line sputter tool from Leybold Optics (A600V7). A laser patterning system from Rofin-Baasel is used for scribing of 1 cm^2 cells and mini modules. For I–V measurements of laser scribe defined solar cells and modules, carefully calibrated dual-source class AAA solar simulator (Wacom WXS-155 S-L2) and a class AAA Xenon flasher (h.a.l.m.) are used. The flasher is equipped with halogen lamps to bias the Xenon lamp spectrum for accurate tandem measurements. Solar cells and modules are light soaked in a temperature controlled (50 °C) light-soaking bench at 1 sun, with a light source calibrated to obtain the AM1.5 a-Si:H top cell current. Generally, cells and mini modules are light soaked for one week (168 h), after which they are close to stabilization.

In order to keep track on the performance of the equipment and processes and for having a stable reference process for experiments, an a-Si:H/μc-Si:H baseline process is maintained at PVcomB. For this baseline commercial SnO$_2$:F (FTO) coated 3.2-mm-thick low-iron float glass, the same as used in production at Masdar PV, is used as the transparent conducting oxide (TCO) substrate material. Intrinsic a-Si:H and μc-Si:H layers for solar cells are deposited at substrate temperatures of approximately 200 °C at rates of 0.22 and 0.45 nm/s, respectively. The i-layer thickness of the top and bottom cells is 270 nm and 1800 nm, respectively. The IV parameters of solar cells made with the baseline process are shown in Fig. 1. The efficiency is distributed in a narrow range around 11.5% (initial), and 10.0% after light soaking. The results shown in Fig. 1 will be further discussed in Section 3. Encapsulated 30 × 30 cm^2 baseline modules (756 cm² aperture area) are routinely made with an initial efficiency of 10.6% (J_{sc} = 10.6 mA/cm², V_{oc} = 1414 mV, FF = 70.5%) and 9.5% (J_{sc} = 10.3 mA/cm², V_{oc} = 1385 mV, FF = 66%) after light soaking. Recently, we optimized the baseline process introducing 230 nm and 1600 nm as the top and bottom i-layer thickness, respectively, yielding slightly improved performance. On ZnO:Al front TCO such 30 × 30 cm^2 modules reach an initial efficiency of 11.7% and 10.3% after light soaking (Fig. 2). Here, a textured light trapping anti reflection (AR) foil from DSM (former Solarexcel) [25] was applied on the front side of the glass.

At Masdar PV the stabilized total-area efficiency of 1.4 m² modules could be increased from below 9% to close to 10% in
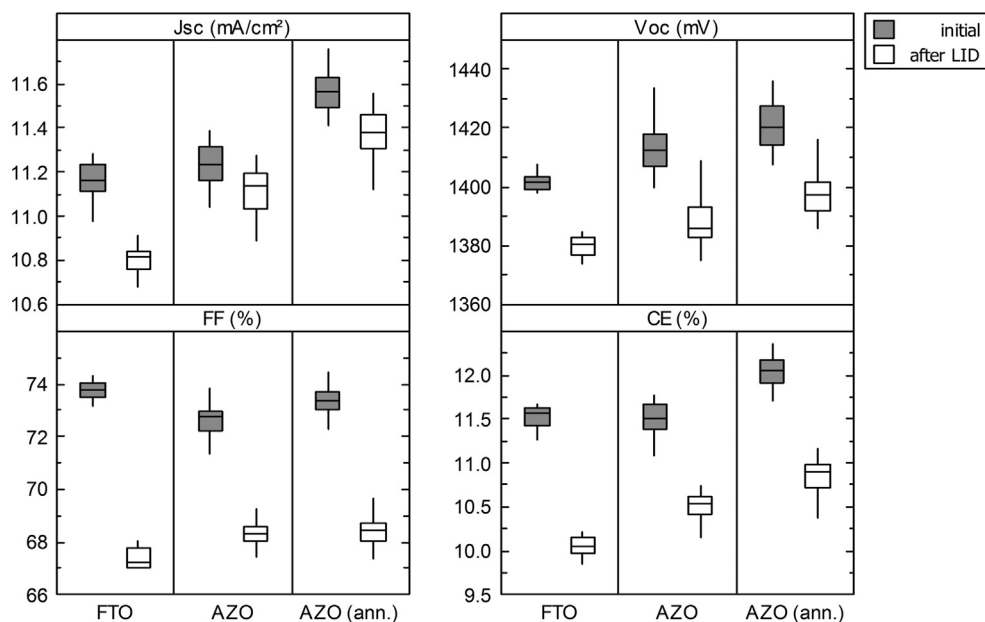

Fig. 1. *IV parameters of a-Si:H/μc-Si:H 1 cm^2 solar cells on different TCOs (compare Table 1): Commercial FTO, industrial AZO type 1, annealed AZO type 1. The same silicon layer thicknesses and deposition rates as indicated in the text are used for cells on all TCOs. Data is shown initially and after one week of light soaking (1 sun, 50 °C). Boxes contain 50% of the data points around the median value (indicated by a line), the whiskers cover 80% of the data points.*
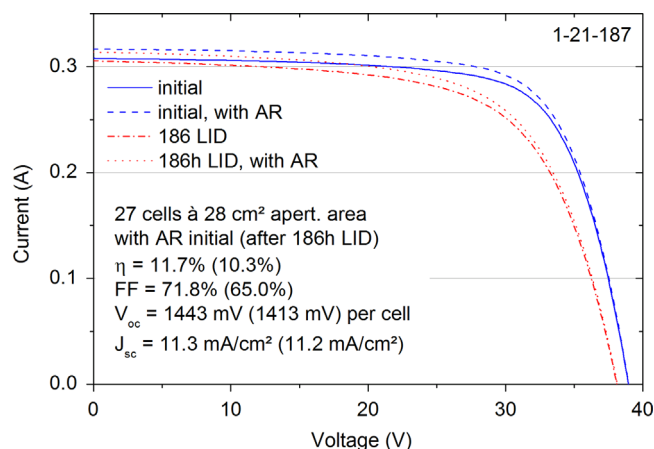
Fig. 2. IV curve of a fully integrated and encapsulated 30×30 cm^2 a-Si:H/μc-Si:H tandem module on AZO front TCO produced on the R & D line at PVcomB, measured initially and after light soaking.
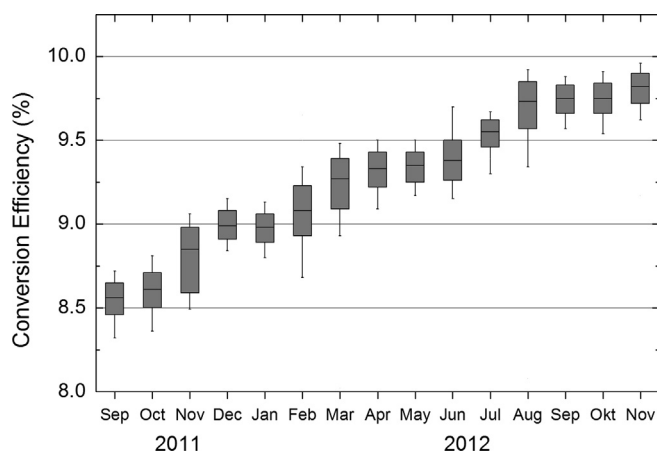

Fig. 3. Development of the stable total area conversion efficiency of 1.43 m^2 a-Si:H/μc-Si:H tandem modules at Masdar PV's production line. Boxes are explained in Fig. 1.

production average, within one year only (Fig. 3). This fast ramping and process integration leading to the high module performance has been made possible by continuous process improvement as well as by the joint development work with systematic development and pre-optimization of PECVD processes at PVcomB. Here, we focused on optimized p-type window layers, implementation of μc-SiO$_x$:H based n- and p-type doped layers, improvement of a-Si:H and μc-Si:H intrinsic layers with respect to module performance and gas consumption. This will be discussed below. The development of advanced TCO substrates is discussed in the next section. To support the process transfer, regular sampling of mini modules from production modules for systematic analysis by I–V characteristics, quantum efficiency, light soaking, Raman spectroscopy and optical R/T spectrophotometry at PVcomB and benchmarking with results of the in-house (baseline) cells and mini modules is carried out.

The PECVD process of all silicon layers in the solar cell device has been investigated at PVcomB in detail. Single layers were deposited on float glass and their optical, electrical and structural properties measured ex situ by various techniques such as spectrophotometry and Raman spectroscopy. A knowledge data base has been built up containing the thin film properties and the deposition processes including data from in situ plasma diagnostics measured during PECVD. An example is the deposition of intrinsic μc-Si:H material, which is implemented as the absorber layer in the bottom cell of a tandem junction [26–28]. The challenge is the

deposition of device quality μc-Si:H material under high deposition rates using low process gas flow rates. However, the process window for device quality μc-Si:H is very small [26,29] and the optimum SiH$_4$/H$_2$ process gas flow rates and their ratio depend strongly on other process parameters such as the gas pressure and the radio frequency (RF) plasma power. We used in situ plasma diagnostics for a detailed scan of the PECVD under various process parameters. From etch product detection [29] and measured time-resolved plasma parameters, the optimized PECVD process windows were developed using less SiH$_4$ process gas and with improved electrical properties in solar cell device.

Another example is μc-SiO$_x$:H, a material recently introduced for wide band gap doped layers, replacing conventional a-SiC:H and μc-Si:H n- and p-type layers, and as low refractive index intermediate reflector layers in thin film silicon solar cells [30–32]. It is a two phase material consisting of (doped) μc-Si:H and amorphous silicon oxide (a-SiO$_x$:H), both with different electrical and optical properties. The structure and composition of μc-SiO$_x$:H depend strongly on the deposition process parameters during PECVD. The impact of these process parameters on the film properties and their influence in the tandem cell device was investigated in detail at PVcomB's PECVD cluster tool [33]. After optimization, the PECVD processes were transferred to the large area production tools at Masdar PV using the process understanding built up during the R & D process at PVcomB. Except for the top-cell p layer on FTO, all doped layers in our solar cell devices are made from μc-SiO$_x$:H material, as it exhibits less parasitic absorption. As a result, the median efficiency of 1.4 m^2 production modules at Masdar PV has been improved from 8.6% in September 2011 to 9.8% in November 2012, which is among the highest values obtained in a-Si:H/μc-Si:H tandem module production. This clearly demonstrates that the a-Si:H/μc-Si:H module technology is mature and robust enough to allow fast process integration on very large scale of 5.7 m^2 module size and, secondly, that process transfer and scaling from-lab-to-fab is possible on a timescale of a few months. Process development is ongoing to increase the module efficiency even further and will focus on the TCO/p contact and advanced light management schemes, including front and back contacts, with FTO as the TCO substrate on the short term. The work on advanced TCO materials, carried out in a funded R & D project, is addressed in the next section.

3. Advanced TCO substrates

An optimized TCO substrate is extremely important for a-Si:H/μc-Si:H modules with high conversion efficiency, suitable for low cost mass production. High transparency over a wide wavelength range of ideally 300–1100 nm and high electrical conductivity with low free-carrier absorption, hence, high carrier mobility are essential. Since up to now light trapping in the silicon absorber layer is achieved predominantly by light scattering at the TCO/silicon interface, the TCO surface topography has to lead to maximum light scattering into the silicon [34,35] and simultaneously allowing for silicon film growth with low (structural) defect density. This has been addressed already in the early 90s by the group of Sato et al. from ASAHI Glass [36] and is subject of present research [37]. In addition, the TCO has to withstand the hydrogen-rich plasma conditions during silicon deposition without chemical reduction and form a good electrical contact to the p layer [38–40]. For commercial modules the TCO substrates need to fulfill the requirements for long term stability as tested in accelerated lifetime tests. For large-scale TCO production the non-uniformity of TCO properties, such as conductivity and surface texture, is a critical issue to be solved [41]. Finally, the raw materials used should be abundant and non-toxic [3].

Two types of TCO are generally used for commercial module production: Boron-doped zinc oxide (ZnO:B or BZO) and fluorine-doped tin oxide (SnO$_2$:F or FTO). Both are natively textured films generally fulfilling the above summarized requirements. BZO is deposited by low-pressure chemical vapor deposition (LPCVD) at moderate temperatures of 150–200 °C [42,43] at typical thicknesses of 1.5–2.5 μm on areas up to 1.4 m^2. FTO is deposited by atmospheric pressure (AP) CVD at higher temperatures of 500–550 °C typically around 800 nm thick. For commercial production FTO is deposited on 3.2 m width in-line in float glass production, which facilitates low coating costs. On both types of TCO large-scale a-Si/μc-Si modules with stabilized efficiencies above 10% were reported, on BZO by Oerlikon Solar [16] and for FTO, e.g. in [15] and in this paper.

As another TCO type, magnetron-sputtered aluminum-doped zinc oxide (ZnO:Al or AZO) has been developed. Etching in diluted HCl or other etching solutions is used for texturing the flat as-deposited surface. While the superior properties for μc-Si based solar cells were demonstrated on RF sputtered ("lab-type") AZO first [44–47], a successful transfer to industrial production using DC sputtering at high deposition rates on an area up to 5.7 m^2 was achieved more recently [48]. Tandem modules on this TCO with stabilized efficiencies above 10% were demonstrated for 1.4 m^2 prototype modules [17]. Up to date, however, AZO is not used in commercial module production since it could not been shown that the higher TCO costs can be compensated by a higher module efficiency, as compared to the established alternatives FTO and BZO.

Comparable tandem efficiencies are obtained on all three types of TCO, reaching around 12% for lab cells and 10–11% for large scale modules, as discussed above. Different TCOs, however, lead to a different distribution of cost contributions in module production. In general, the TCO contributes significantly to the total module costs with typically 2–6 €/m^2 coating costs, which account for significant 2–6 €-cent per W$_p$ assuming modules with 10% conversion efficiency [48]. Fig. 4 displays the relative cost contributions for tandem modules based on FTO as produced at Masdar PV. Raw materials account for about 42% of the total costs, from which about 30% is ascribed to the FTO coated glass substrate. FTO can be produced at relatively low costs, as explained above, but, due to poorer light scattering properties, the intrinsic silicon layers have to be relatively thick (typically 1.4–1.8 μm thickness of μc-Si:H) for high efficiency. This results in higher silicon-related costs, namely, PECVD costs (part of "equipment" in Fig. 4a) and raw materials like SiH$_4$ and NF$_3$ gas (part of "CVD" in Fig. 4b). BZO, in contrast, offers better light scattering which allows for thinner silicon layers, in production typically only around 200 nm for the a-Si:H top cell i-layer and 800 nm for the μc-Si:H bottom cell i-layer, as proposed by Oerlikon Solar (now: Tokyo Electron Solar) for the "ThinFab" production line. This allows for reduced PECVD costs. To obtain this superior light scattering, however, the TCO has to be > 1.5 μm thick, which hinders low TCO costs. In conclusion, for high efficiency modules at lowest possible costs, a *thin* TCO that facilitates also *thin* silicon layers is needed.

At PVcomB we use all three types of TCO for solar cell development [49]. Fig. 5 shows the surface topography of the above discussed TCOs, as used for solar cell development at PVcomB. The TCO properties are summarized in Table 1. The commercial FTO shown is used for production at Masdar PV and the baseline process at PVcomB. Outstanding is the high carrier mobility, which is only outperformed by annealed AZO, as discussed below. The relatively small feature size is comparable to the smaller crater size for the DC sputtered AZO type 1, used for solar cells as discussed below. As a result, good scattering in the short-wavelength range (absorbed in the top cell) is obtained while the scattering in the long-wavelength range (absorbed in the bottom
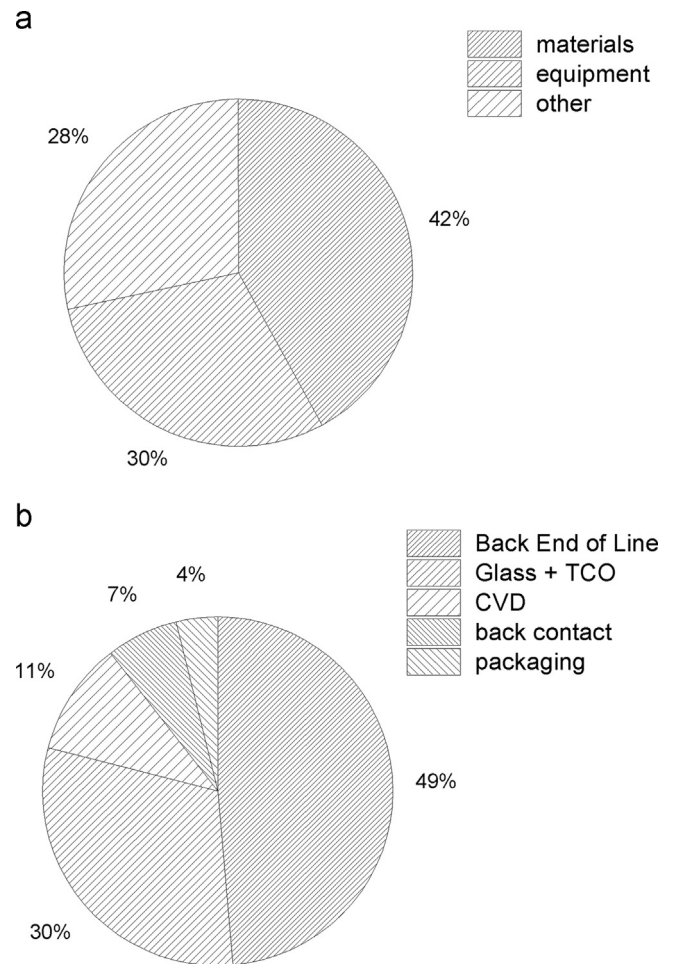
a

b

Fig. 4. Relative cost allocation for a-Si:H/μc-Si:H module production: Total module costs (a) and the materials costs only (b) (data from Masdar PV). Equipment costs contain depreciation and maintenance.

cell) is lower. For comparison another DC sputtered AZO (type 2) with larger crater size comparable to those obtained in the lab with RF sputtered AZO [47] and a production-type BZO is shown. Solar cell development on these TCO substrates is not discussed within this paper.

At PVcomB the highest tandem cell efficiencies are currently obtained on AZO, originating from a large-area production line. Tandem cells consist of 260–290 nm thick a-Si:H top cell i layers and 1800 nm thick μc-Si:H bottom cell i layers with all doped layers based on μc-SiO$_x$:H. Cells are deposited on 700 nm thick DC-sputtered ZnO:Al on low-iron float glass (type 1). Surface texture is obtained by the commonly used etching in diluted HCl resulting in a surface morphology as shown in Fig. 5 (bottom left). The potential of this TCO has been demonstrated by Klein et al. with large scale tandem modules reaching > 10% stable efficiency [17]. We continued the cell and module development on this TCO and, additionally, implemented a thermal annealing process as reported previously [50,51]. Annealing under an a-Si:H capping layer at around 500 °C for several hours leads to an increased transparency, predominantly in the short wavelength range and an increased carrier mobility from typically 20–30 cm^2/Vs for as deposited layers to well above 60 cm^2/Vs (Table 1) [52]. This mobility is among the highest values reported for sputtered ZnO:Al [50,53], and allows for reduction of either the carrier density, hence, the free-carrier absorption in the NIR part of the spectrum, or the TCO thickness, or both. In case of the annealed AZO as shown in Table 1 a two-step annealing process was applied [51,52]: The carrier density was reduced by a first annealing step
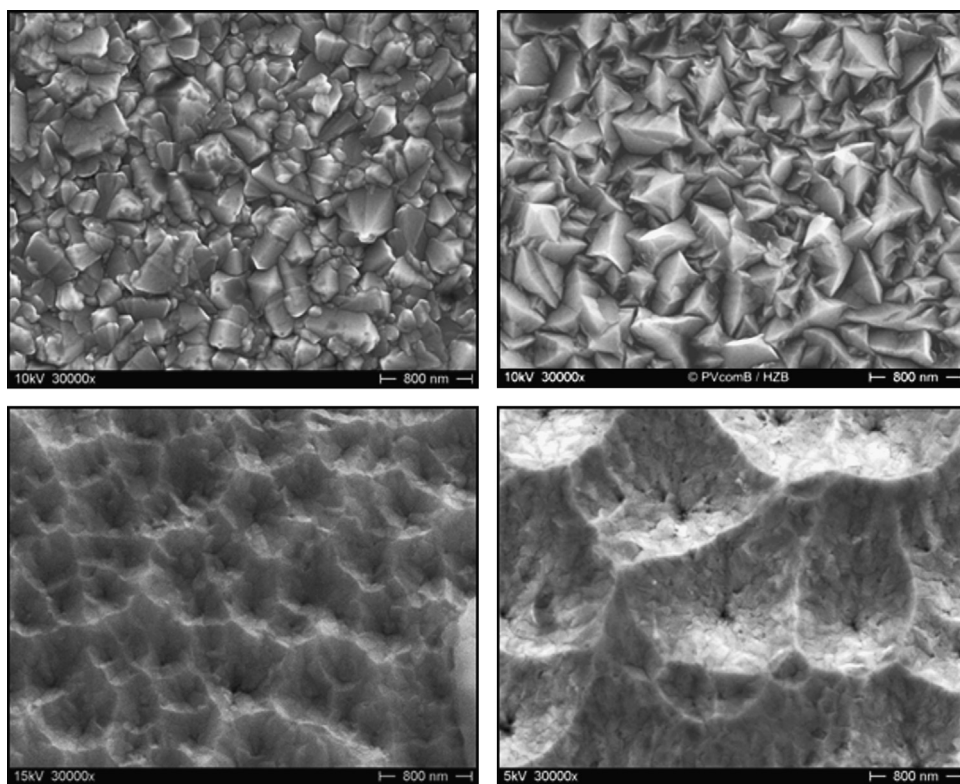
Fig. 5. Scanning electron microscope (SEM) images of commercial FTO (top left), production-type BZO (top right), DC sputtered AZO "type 1" (bottom left), and DC sputtered AZO "type 2" (bottom right). The AZO based TCOs were texture-etched in diluted HCl.

Table 1
Properties of TCOs as used at the PVcomB. In the case of AZO, properties are measured after texture etching. Surface morphologies of some of the samples are given in Fig. 5.

TCO type	d (nm)	R_{sheet} (Ω)	μ_{Hall} (cm^2/Vs)	haze@700 nm (%)
Commercial FTO	800	11.5	41	6.7
DC sputtered AZO "type 1"	700	12.0	23	8.6
DC sputtered AZO "type 1" (annealed)	650	10.0	60	9.7
DC sputtered AZO "type 2"	650	10.9	30	54
RF sputtered AZO ("lab type")	650	6.4	32	67
BZO ("production type")	1600	18.5	27	11.7

Fig. 6. Conversion efficiency of a-Si:H single junction and a-Si:H/μc-Si:H tandem junction solar cells and mini modules deposited at PVcomB. Data from 1 cm^2 solar cells (active area) and mini modules (12 cells à 6.6-mm-wide and 8-cm-long, aperture area) upon light soaking (1 sun, 50 °C) is shown. Single junctions are based on AZO type 1 and tandem junctions are based on annealed AZO type 1 (Table 1).

without capping. Subsequently, the carrier mobility was increased in a second annealing step performed with an a-Si:H capping layer. As a consequence, in total the sheet resistance was kept almost unchanged, while the transparency increased over the entire spectral range. Both the improved transparency for short wavelengths and the enhanced carrier mobility are ascribed to a reduction of grain boundary defects as a consequence of the annealing process [54].

The IV parameters of cells on FTO (PVcomB baseline process), AZO and annealed AZO are shown in Fig. 1. Except for the top cell p layer, which has been adjusted to the specific TCO, the cell design and the PECVD process are the same for the cells on the three TCOs. All cells are slightly top cell current limited. Generally, the cells on AZO show better (stable) performance than the cells on FTO. Since the opto-electronical properties of both TCOs are comparable, we ascribed this difference mainly to the better electrical and optical performances of the μc-SiO$_x$:H top cell p layer on AZO [17,32], as compared to the a-SiC:H p layer used for cells on FTO. When comparing AZO with annealed AZO, an improvement of 0.4–0.5% (abs.) can be found in the cell efficiency
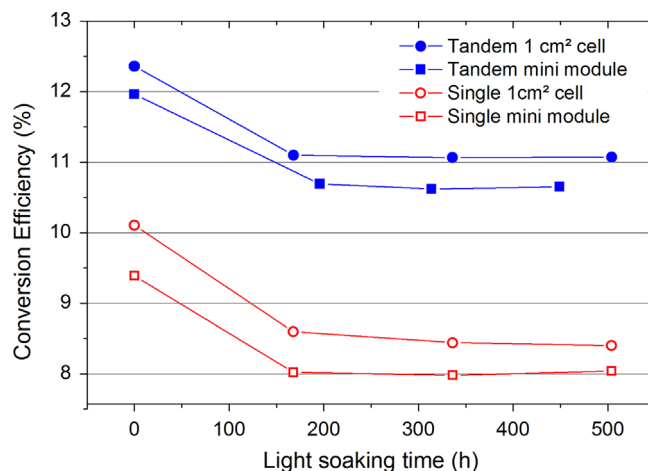
on the latter. In the first place, this is due to an improved transparency over the entire spectral range, as mentioned above. Moreover, a slight improvement of fill factor and open circuit voltage is observed [52]. The reason for this is unknown, but most likely due to an improved TCO/p contact. Tandem cells with this process reach an efficiency of 12.4% (initial) and 11.1% (stable). The efficiency development upon light soaking of cells and mini modules on annealed AZO together with those of a-Si:H single junctions on as-deposited (not annealed) AZO are shown in Fig. 6. As can be seen, the efficiency of solar cells and mini modules has almost stabilized already after one week of light soaking.

Table 2
Parameters of champion solar cell and mini modules measured initial and after light-induced degradation (LID, 1 sun, 50 °C). Devices are deposited with identical processes on annealed AZO on 3.2 mm low iron glass with textured light trapping foil (DSM) on front side.

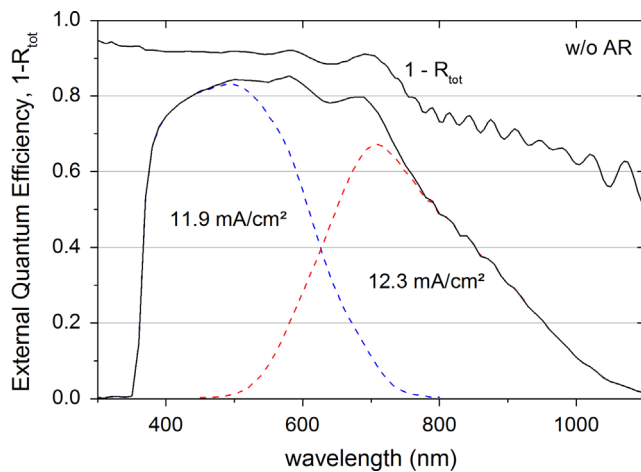|		**LID** (h)	η (%)	V_{oc} (mV)	J_{sc} (mA/cm^2)	**FF** (%)
solar cell	1 cm^2 active area	0	13.3	1432	12.7	73.2
		995	12.1	1411	12.6	67.8
module	12 cells, 63.4 cm^2 apert. area	0	12.8	1425	12.3	72.8
		939	11.6	1414	12.1	68.0
module	41 cells, 757.7 cm^2 apert. area	0	12.2	1443	11.8	71.3
		454	10.6	1412	11.6	64.5

Fig. 7. External Quantum Efficiency and $1 - R_{tot}$ (total reflection) of an optimized a-Si:H/µc-Si:H tandem cell on annealed AZO, IV parameters as shown in Table 2.

Recently, we improved the solar cell process on annealed AZO. The µc-SiO$_x$:H based top cell p layer was further optimized according to [32] and the µc-SiO$_x$:H intermediate reflector thickness was increased from 45 to 60 nm. As a consequence of that and due to the modest light scattering in the NIR the bottom cell thickness had to be increased to 2800 nm to obtain current matching. This yielded 1 cm^2 cells with an efficiency of 13.3%, initial, and 12.1% after stabilization (Table 2). Cells were measured with textured light trapping AR foil as mentioned above. The external quantum efficiency of this cell (measured without textured light trapping foil) is shown in Fig. 7. As a result of the annealed AZO and the optimized µc-SiO$_x$:H p layer, the top cell exhibits a remarkable high blue response.

For 10 × 10 cm^2 mini modules with 12 cells of a width of 6.6 mm, optimized with respect to the TCO sheet resistance, and a narrow interconnect width ("dead area") of approximately 130 µm, this resulted in an initial efficiency of 12.8% and 11.6% after 939 h of light soaking. For 30 × 30 cm^2 modules 12.2% (initial) and 10.6% (stable) are obtained (Table 2).

4. Perspectives for thin film silicon solar modules

To increase the stabilized tandem module efficiency well beyond 12% two major limitations need to be overcome: the weak light absorption in µc-Si:H due to its indirect band gap and the light induced degradation of a-Si:H (and a-SiGe:H) solar cells due to the Staebler–Wronski-Effect (SWE) [55]. To cope with both of these drawbacks advanced light-trapping schemes were developed and successfully implemented, resulting in total current

densities (the sum of all junctions) almost reaching 30 mA/cm^2 for tandem junctions [22,23,56] and triple junctions [18,24,57]. Even though it is remarkably high, this is still only 2/3 of the theoretical maximum of about 43.5 mA/cm^2 for crystalline silicon. The missing part is lost due to light reflection out of the cell and parasitic absorption, predominantly in the TCO front contact. The above mentioned record solar cells exhibit initial efficiencies reaching the highest reported value of 16.3% for a n-i-p type triple cell by the Uni Solar group [57]. This efficiency value, however, degrades due to the SWE. Unraveling the microscopic defect-creation mechanisms in a-Si:H and finding methods to circumvent this effect are subject of present work, e.g. in [21,58]. Unless the SWE can be solved or alternative, stable high and medium band gap materials are found, two scenarios—or a combination of both—are possible: Firstly, revolutionary new light trapping schemes facilitating total currents well above 30 mA/cm^2 for thin solar cells are developed (e.g. [59–61]). As an example, attempts are being made to de-couple the light scattering from the TCO deposition, e. g. by nano-imprinting of scattering structures [62] or textured glass [22,63]. At PVcomB further improvement of the above discussed annealed AZO, combining a thin (< 400 nm) annealed AZO with a scattering superstrate is the subject of current research [64]. This could be the TCO substrate of choice for high efficiency with thin TCO and thin silicon layer thicknesses, hence, allowing for low production costs. For the second scenario, high-quality silicon layers in the range of 10 µm and more need to be employed. To date this is not a feasible, low-cost route for a-Si:H/µc-Si:H based solar cells due to the low deposition rate of 0.5–1 nm/s for high quality µc-Si:H layers on production-scale equipment that is available. Other, high rate thin-film Si material needs to be developed. As a possible candidate poly-Si is discussed in a contribution in this issue [65].

5. Summary and conclusions

This paper briefly reviews the achievements of the a-Si:H/µc-Si tandem solar cell technology, from the early work in the 90s until mass production in the last years. As an example we show key figures of the module production at Masdar PV, with large-scale module conversion efficiency of 10%. The fast process integration in only one year demonstrates the mature technology and the effective process transfer from lab to fab. The important role of the TCO substrate for producing high-efficiency modules at lowest possible costs is discussed. Results of the tandem baseline and high efficiency solar cells and mini modules on advanced TCO substrates at PVcomB are presented. As an example, we discuss tandem cells on thermally annealed ZnO:Al substrates, resulting in an improvement of 0.4–0.5% (abs) as a result of the TCO annealing, reaching a stable efficiency of 12.1% for a 1 cm^2 cell. Best mini modules recently have reached 12.8% initial efficiency and 11.6% after light soaking. Generally, it will be challenging to increase module efficiency even further beyond 12%, since limitations exist in lab cells. Ways to increase cell efficiency significantly are fundamentally new light management schemes or poly-Si on glass. Both are subject of intense R & D work that is ongoing.

References

[1] A. Jäger-Waldau, PV Status Report, Scientific and Policy Report by the Joint Research Center of the European Commission, 2012.
[2] Photon International, 3, Quarter, 2012, p. 142.
[3] A. Feltrin, A. Freundlich, Material considerations for terawatt level deployment of photovoltaics, Renewable Energy 33 (2) (2008) 180–185.
[4] A.Virtuani, D. Pavanello, G. Friesen, Overview of temperature coefficient of different thin film photovoltaic technologies in: Proceedings of the 25th EU Photovoltaic Solar Energy Conference and Exhibition, 5th World Conference on Photovoltaic Energy Conversion, Valencia, Spain, 2010, pp. 4248–4252.
[5] J.A. del Cueto, B. von Roedern, Temperature-induced changes in the performance of amorphous silicon multi-junction modules in controlled light-soaking, Progress in Photovoltaics: Research and Applications 7 (1999) 101–112.
[6] R. Ruther, J. del Cueto, G. Tamizh-Mani, A. Montenegro, S. Rummel, A. Anderberg, B. von Roedern, Proceedings of the 33rd IEEE Photovoltaic Specialists Conference, 2008, pp. 1–5.
[7] A. Shah, P. Torres, R. Tscharner, N. Wyrsch, H. Keppner, Photovoltaic technology: the case for thin-film solar cells, Science 285 (1999) 692.
[8] B. Rech, H. Wagner, Potential of amorphous silicon for solar cells, Applied Physics A 69 (1999) 155–167.
[9] B. Rech, T. Roschek, T. Repmann, J. Müller, R. Schmitz, W. Appenzeller, Microcrystalline silicon for large area thin film solar cells, Thin Solid Films 427 (2003) 157–165.
[10] J. Meier, P. Torres, R. Platz, S. Dubail, U. Kroll, J.A.A. Selvan, N. Pellaton-Vaucher, C. Hof, D. Fischer, H. Keppner, A. Shah, K.-D. Ufert, P. Giannoules, J. Köhler, On the way towards high efficiency thin film silicon solar cells by the "micromorph" concept, Proceedings of the Materials Research Society Symposium 420 (1996) 3–14.
[11] M.A. Green, K. Emery, Y. Hishikawa, W. Warta, E.D. Dunlop, Solar cell efficiency tables (version 41), Progress in Photovoltaics: Research and Applications 21 (2013) 1–11.
[12] K. Yamamoto, M. Yoshimi, Y. Tawada, Y. Okamoto, A. Nakajima, Cost effective and high-performance thin film Si solar cell towards the 21st century, Solar Energy Materials and Solar Cells 66 (2001) 117–125.
[13] K. Yamamoto, A. Nakajima, M. Yoshimi, T. Sawada, S. Fukuda, T. Suezaki, M. Ichikawa, Y. Koi, M. Goto, T. Meguro, T. Matsuda, M. Kondo, T. Sasaki, Y. Tawada, A high efficiency thin film silicon solar cell and module, Solar Energy 77 (2004) 939–949.
[14] K. Yamamoto, A. Nakajima, M. Yoshimi, T. Sawada, S. Fukuda, K. Hayashi, T. Suezaki, M. Ichikawa, Y. Koi, M. Goto, H. Takata, Y. Tawada, Proceedings of the 29th IEEE Photovoltaic Specialists Conference, 2002, pp. 1110–1113.
[15] J. Springer, T. Dittkrist, D. Hrunski, J. Pantförder, S. Bönisch, T. Bergmann, F. Lindner, A. Katzung, J. Rittner, F. Schöne1, M. Vouters, R. Hesse, T. Liebschner, B. Stannowski, U. Klemm, T. Brammer, T. Hänel, B. Rech, Proceedings of the 25th European Photovoltaic Solar Energy Conference, Valencia, Spain, 2010, p. 2896.
[16] O. Kluth, J. Kalas, M. Fecioru-Morariu, P. A. Losio, J. Hoetzel, Proceedings of the 26th European Photovoltaic Solar Energy Conference, Hamburg, Germany, 2011, p. 2354.
[17] S. Klein, S. Wieder, S. Buschbaum, M. Rohde, K. Schwanitz, T. Stolley, C. Stömmer, D. Severin, A. Straub, U.I. Schmidt, K. Ahmed, Large area thin film silicon modules with 10% efficiency for production, Physica Status Solidi C 8 (10) (2011) 2978–2981.
[18] S. Kim, J-W. Chung, H. Lee, J. Park, Y. Heo, H-M. Lee, Remarkable progress in thin-film silicon solar cells using high-efficiency triple-junction technology, Solar Energy Materials and Solar cells, http://dx.doi.org/10.1016/j.solmat.2013.04.016, this issue.
[19] M. Matsumotoa, Y. Ayaa, M. Hishidaa, S. Yataa, W. Shinoharaa, I. Yoshidaa, D. Kanematsua, A. Terakawaa, M. Isekia, M. Tanakaa, Proceedings of the MRS Spring Meeting, vol. 1426, 2012.
[20] M. Despeisse, M. Boccard, C. Battaglia, G. Bugnon, M. Charrière, L. Garcia, M. Bonnet-Eymard, J. Escarre, P. Cuony, M. Stuckelberger, G. Parascandolo, S. Hänni, L. Löfgren, J.-W. Schüttauf, L. Ding, S. Nicolay, F. Meillaud, C. Ballif, Proceedings of 38th IEEE Photovoltaic Specialists Conference, Austin, Texas, 2012.
[21] T. Matsui, H. Sai, K. Saito, M. Kondo, High-efficiency thin-film silicon solar cells with improved light-soaking stability, Progress in Photovoltaics: Research and Applications (2012), http://dx.doi.org/10.1002/pip.2300.
[22] U. Kroll et al., Recent development of high-efficiency micromorph tandem solar cells in KAI-M/Plasmabox PECVD reactors, in: Proceedings of the 26th European Photovoltaic Solar Energy Conference, Hamburg, Germany, 2011, p. 2340.
[23] T. Sasaki, N. Kadota, M. Gotoh, K. Shimizu, T. Takahashi, T. Sawada, S. Fukuda, M. Yoshimi, K. Yamamoto, T. Nomura, A. Nakajima, Proceedings of 35th IEEE Photovoltaic Specialists Conference, Hawaii, 2010, pp. 1134–1140.
[24] S. Kim, J. Park, H. Lee, H. Lee, S.-W. Ahn, H.-M. Lee, Microcrystalline silicon carbide p-layer with wide-bandgap and its application to single- and triple-junction silicon thin-film solar cells, Japanese Journal of Applied Physics 51 (2012) 1–4 10NB11.
[25] C. Ulbrich, A. Gerber, K. Hermans, A. Lambertz, U. Rau, Analysis of short circuit current gains by an anti-reflective textured cover on silicon thin film solar cells, Progress in Photovoltaics: Research and Applications (2012), http://dx.doi.org/10.1002/pip.2249.
[26] O. Vetterl, F. Finger, R. Carius, P. Hapke, L. Houben, O. Kluth, A. Lambertz, A. Mück, B. Rech, H. Wagner, Intrinsic microcrystalline silicon: a new material for photovoltaics, Solar Energy Materials and Solar Cells 62 (2000) 97–108.
[27] M. Kondo, M. Fukawa, L. Guo, A. Matsuda, High rate growth of microcrystalline silicon at low temperatures. Journal of Non-Crystalline Solids 266–269 (2000) 84–89.
[28] J. Meier, U. Kroll, E. Vallat-Sauvain, J. Spitznagel, U. Graf, A. Shah, Amorphous solar cells, the micromorph concept and the role of VHF-GD deposition technique, Solar Energy 77 (2004) 983–993.
[29] G. Dingemans, M.N. van den Donker, D. Hrunski, A. Gordijn, W.M.M. Kessels, M.C.M. van de Sanden, The atomic hydrogen flux to silicon growth flux ratio during microcrystalline silicon solar cell deposition, Applied Physics Letters 93 (2008) 111914.
[30] A. Lambertz, T. Grundler, F. Finger, Hydrogenated amorphous silicon oxide containing a microcrystalline silicon phase and usage as an intermediate reflector in thin-film silicon solar cells, Journal of Applied Physics 109 (2011) 113109.
[31] P. Cuony, D.T.L. Alexander, I. Perez-Wurfl, M. Despeisse, G. Bugnon, M. Boccard, T. Söderström, A. Hessler-Wyser, C. Hébert, C. Ballif, Silicon filaments in silicon oxide for next-generation photovoltaics, Advanced Materials 24 (2012) 1182–1186.
[32] K. Schwanitz, S. Klein, T. Stolley, M. Rohde, D. Severin, R. Trassl, Anti-reflective microcrystalline silicon oxide p-layer for thin-film silicon solar cells on ZnO, Solar Energy Materials and Solar Cells 105 (2012) 187–191.
[33] S. Kirner, O. Gabriel, B. Stannowski, B. Rech, R. Schlatmann, The growth of microcrystalline silicon oxide thin films studied by in situ plasma diagnostics, Applied Physics Letters 102 (2013) 051906.
[34] J. Müller, B. Rech, J. Springer, M. Vanecek, TCO and light trapping in silicon thin film solar cells, Solar Energy 77 (6) (2004) 917–940.
[35] M. Berginski, J. Hüpkes, M. Schulte, G. Schöpe, H. Stiebig, B. Rech, M. Wuttig, The effect of front ZnO:Al surface texture and optical transparency on efficient light trapping in silicon thin-film solar cells, Journal of Applied Physics 101 (2007) 074903.
[36] K. Sato, Y. Gotoh, Y. Wakayama, Y. Hayashi, K. Adachi, H. Nishimura, Highly textured SnO2:F TCO films for a-Si solar cells, Reports of the Research Laboratory, Asahi Glass Co., Ltd. 42 (1992) 129–137.
[37] G. Bugnon, G. Parascandolo, T. Söderström, P. Cuony, M. Despeisse, S. Hänni, J. Holovský, F. Meillaud, C. Ballif, A new view of microcrystalline silicon: the role of plasma processing in achieving a dense and stable absorber material for photovoltaic applications, Advanced Functional Materials 22 (2012) 3665–3671.
[38] H. Schade, Z.E. Schmidt, J.H. Thomas III, A. Catalano, Hydrogen plasma interaction with tin oxide surfaces, Thin Solid Films 117 (1984) 149–155.
[39] T. Minami, H. Sato, H. Nanto, S. Takata, Heat treatment in hydrogen gas and plasma for transparent conducting oxide films such as ZnO, SnO2 and indium tin oxide, Thin Solid Films 176 (1989) 277–282.
[40] S. Hegedus, Characterization of the SnO2/p and ZnO/p contract resistance and junction properties in a–Si p-i-n solar cells and modules, Journal of Applied Physics 92 (2002) 620–623.
[41] S. Ring, F. Säuberlich, T. Wendelmuth, B. Stannowski, V. Sittinger, B. Szyszka, Proceedings of 25th European Photovoltaic Solar Energy Conference, Valencia, Spain, 2010.
[42] S. Faÿ, L. Feitknecht, R. Schlüchter, U. Kroll, E. Vallat-Sauvain, A. Shah, Rough ZnO layers by LP-CVD process and their effect in improving performances of amorphous and microcrystalline silicon solar cells, Solar Energy Materials Solar Cells 90 (2006) 2960–2967.
[43] L. Ding, M. Boccard, G. Bugnon, M. Benkhaira, S. Nicolay, M. Despeisse, F. Meillaud, C. Ballif, Highly transparent ZnO bilayers by LP-MOCVD as front electrodes for thin-film micromorph silicon solar cells, Solar Energy Materials and Solar Cells 98 (2012) 331–336.
[44] A. Löffl, S. Wieder, B. Rech, O. Kluth, C. Beneking, H. Wagner, Proceedings of the 14th European Photovoltaic Solar Energy Conference, Barcelona, Spain, 1997.
[45] J.A.A. Selvan, ZnO for thin film solar cells, Université de Neuchâtel, Switzerland, 1998. (Ph.D. thesis).
[46] O. Kluth, B. Rech, L. Houben, S. Wieder, G. Schöpe, C. Beneking, H. Wagner, A. Löffl, H.W. Schock, Texture etched ZnO:Al coated glass substrates for silicon based thin film solar cells, Thin Solid Films 351 (1999) 247–253.
[47] M. Berginski, J. Hüpkes, W. Reetz, B. Rech, M. Wuttig, Recent development on surface-textured ZnO:Al films prepared by sputtering for thin-film solar cell application, Thin Solid Films 516 (2008) 5836–5841.
[48] C. Daube, U.I. Schmidt, D. Severin, Ch. Kurthen, C. Goergens, K. Ahmed, I. Vermeir, N. Kuhr, S. Klein, A. Straub, S. Wieder, D. Forster, Th. Zilbauer, A. Rembeck, R. Schubert, M. Rohde, Ch. Stömmer, Th. Deppisch, Proceedings of 25th European Photovoltaic Solar Energy Conference, Valencia, Spain, 2010, p. 2771.
[49] S. Calnan, S. Neubert, C. Nock, O. Gabriel, M. Rohde, F. Ruske, B. Stannowski, R. Schlatmann, Proceedings of 37th Photovoltaic Specialists Conference PVSC, 2011.
[50] F. Ruske, M. Roczen, K. Lee, M. Wimmer, S. Gall, J. Hüpkes, D. Hrunski, B. Rech, Improved electrical transport in Al-doped zinc oxide by thermal treatment, Journal of Applied Physics 107 (2010) 013708.

[51] M. Wimmer, F. Ruske, S. Scherf, B. Rech, Improving the electrical and optical properties of DC-sputtered ZnO:Al by thermal post deposition treatments, Thin Solid Films 520 (2012) 4203–4207.

[52] S. Neubert, M. Wimmer, F. Ruske, S. Calnan, O. Gabriel, B. Stannowski, R. Schlatmann, B. Rech, Improved conversion efficiency of a-Si:H/μc-Si:H thin-film solar cells by using annealed Al-doped zinc oxide as front electrode material, , Progress in Photovoltaics: Research and Applications (2013), http://dx.doi.org/10.1002/pip.2389.

[53] M. Warzecha, J.I. Owen, M. Wimmer, F. Ruske, J. Hotovy, J. Hüpkes, High mobility annealing of transparent conductive oxides, IOP Conference Series: Materials Science and Engineering 34 (2012) 012004–012018.

[54] F. Ruske, M. Wimmer, G. Köppel, A. Pflug, B. Rech, Optical characterization of high mobility polycrystalline ZnO:Al films, in: Proceedings of SPIE, Oxide-based Materials and Devices III, vol. 8263, 2012, p. 826303.

[55] D.L. Staebler, C.R. Wronski, Reversible conductivity changes in discharge-produced amorphous Si, Applied Physics Letters 31 (4) (1977) 292–294.

[56] M. Boccard, C. Battaglia, S. Hänni, K. Söderström, J. Escarré, S. Nicolay, F. Meillaud, M. Despeisse, C. Ballif, Multiscale transparent electrode architecture for efficient light management and carrier collection in solar cells, Nano Letters 12 (2012) 1344–1348.

[57] B. Yan, G. Yue, L. Sivec, J. Yang, S. Guha, C.-S. Jiang, Innovative dual function nc-SiOx:H layer leading to a >16% efficient multijunction thin-film silicon solar cell, Applied Physics Letters 99 (2011) 113512.

[58] M. Fehr, A. Schnegg, B. Rech, K. Lips, O. Astakhov, F. Finger, G. Pfanner, C. Freysoldt, J. Neugebauer, R. Bittl, C. Teutloff, Combined multifrequency EPR and DFT study of dangling bonds in a-Si:H, Physical Review B 84 (2011) 1–10 245203.

[59] H.A. Atwater, A. Polman, Plasmonics for improved photovoltaic devices, Nature Materials 9 (2010) 205–213.

[60] G. Brönstrup, N. Jahr, C. Leiterer, A. Csáki, W. Fritzsche, S. Christiansen, Optical properties of individual silicon nanowires for photonic devices, ACS Nano 4 (12) (2010) 7113–7122.

[61] M. Vanecek, O. Babchenko, A. Purkrt, J. Holovsky, N. Neykova, A. Poruba, Z. Remes, J. Meier, U. Kroll, Nanostructured three-dimensional thin film silicon solar cells with very high efficiency potential, Applied Physics Letters 98 (16) (2010) 163503.

[62] C. Battaglia, J. Escarre, K. Söderström, L. Erni, L. Ding, G. Bugnon, A. Billet, M. Boccard, L. Barraud, S. De Wolf, F.-J. Haug, M. Despeisse, C. Ballif, Nanoimprint lithography for high-efficiency thin-film silicon solar cells, Nano Letters 11 (2) (2011) 661–665.

[63] J. Steinhauser, J.-F. Boucher, E. Omnes, D. Borrello, E. Vallat-Sauvain, G. Monteduro, M. Marmelo, J.-B. Orhan, B. Wolf, J. Bailat, S. Benagli, J. Meier, U. Kroll, Improving low pressure chemical vapor deposited zinc oxide contacts for thin film silicon solar cells by using rough glass substrates, Thin Solid Films 520 (4), 2011, 1218–1222.

[64] B. Stannowski, F. Ruske, S. Neubert, S. Schönau, S. Ring, S. Calnan, M. Wimmer, O. Gabriel, B. Szyszka, B. Rech, R. Schlatmann, Thin Solid Films (2013). (submitted for publication).

[65] C. Becker, D. Amkreutz, T. Sontheimer, V. Preidel, D. Lockau, J. Haschke, L. Jogschies, C. Klimm, J.J. Merkel, P. Plocica, S. Steffens, B. Rech, Polycrystalline silicon thin-film solar cells: Status and perspectives, Solar Energy Materials and Solar Cells, http://dx.doi.org/10.1016/j.solmat.2013.05.043 (this issue).